sustainability

MDPI

Article

Impact of Urban Climate Landscape Patterns on Land Surface Temperature in Wuhan, China

Yasha Wang [1,2,3], Qingming Zhan [1,2,*] and Wanlu Ouyang [1,2]

1 School of Urban Design, Wuhan University, Wuhan 430072, China; yasha.wang@whu.edu.cn (Y.W.); wanlu.oy@whu.edu.cn (W.O.)
2 Collaborative Innovation Center of Geospatial Technology, Wuhan 430072, China
3 Faculty of Design and Architecture, Zhejiang Wanli University, Ningbo 315100, China
* Correspondence: qmzhan@whu.edu.cn; Tel.: +86-27-8677-3062

Received: 3 August 2017; Accepted: 18 September 2017; Published: 22 September 2017

Abstract: Facing urban warming, mitigation and adaptation strategies are not efficient enough to tackle excessive urban heat, especially at the local scale. The local climate zone (LCZ) classification scheme is employed to examine the diversity and complexity of the climate response within a city. This study suggests that zonal practice could be an efficient way to bridge the knowledge gap between climate research and urban planning. Urban surfaces classified by LCZ are designated as urban climate landscapes, which extends the LCZ concept to urban planning applications. Selecting Wuhan as a case study, we attempt to explore the climatic effect of landscape patterns. Thermal effects are compared across the urban climate landscapes, and the relationships between patch metrics and land surface temperature (LST) are quantified. Results indicate that climate landscape layout is a considerable factor impacting local urban climate. For Wuhan, 500 m is an optimal scale for exploring landscape pattern-temperature relationships. Temperature contrast between surrounding landscape patches has a major influence on LST. Generally, fragmental landscape patches contribute to heat release. For most climate landscape types, patch metrics also have a significant effect on thermal response. When three metrics are included as predictive variables, 53.3% of the heating intensity variation can be explained for the Large Lowrise landscape, while 57.4% of the cooling intensity variation can be explained for the Water landscape. Therefore, this article claims that land-based layout optimization strategy at local scale, which conforms to planning manner, should be taken into account in terms of heat management.

Keywords: urban climate; urban landscape; local climate zone (LCZ); urban heat island (UHI); mitigation and adaptation strategy; urban planning

1. Introduction

Global warming is an indisputable fact, and city temperatures are significantly higher than the global average temperature [1,2]. Urban thermal environment influences residents' health, energy consumption, and so on. The urban heat island (UHI) and related climatic issues have been extensively investigated by global researchers for more than 100 years [3]. Urban surface characteristics are considered to be the main factors affecting UHIs [4–6]. Governing the near-surface energy balance, land surface temperature (LST), derived from remote sensing imagery, modulates the air temperature and thus influences urban microclimate [7–9].

From the perspective of landscape ecology, a large number of studies have examined the relationship between land use/land cover (LULC) spatial distribution and LST [10–13]. However, the conventional LULC classification system is not well suited for urban landscapes. Impervious surface is treated as a single type [13], or may be subdivided into buildings and non-buildings such as

pavement [11,14]. The former approach fails to distinguish the climatic diversity of the urban building environment. Results of later studies are not easily applicable, because urban planning processes focus on land parcels rather than individual buildings. A more reasonable classification system is thus needed.

Mitigation and adaptation strategies are needed to limit potential heat stress risk. Generally, heat management strategies fall into three categories: (1) utilizing green infrastructure to lower the ambient temperature [15–18]; (2) modifying urban form to improve ventilation potential and heat release [19,20]; (3) using advanced technology and materials to cool buildings and the environment [21]. Beyond that, mitigation efforts should consider land-use planning strategies within cities [22], especially in the early stage of the urban planning process.

Local climate zone (LCZ) classification scheme provides a standard method to study the internal climate within cities and divides the urban surface into relatively homogeneous classes at the local scale (10^2–10^4 m) [23]. The LCZ classification distinguishes built environments more finely than other similar classification schemes such as local thermal zone (LTZ) classification [24]. In further studies based on the LCZ scheme, different methods of classification and various data sources are considered in order to achieve better classification results [25,26]. Some researchers focus on the classification results and their accuracy [27–29]. Others have conducted simulation studies based on specific LCZ scenarios [16,30]. Compared with the conventional LULC classification scheme, LCZs are better suitable for the urban planning process due to the zoning practices at the local scale. However, there is little discussion about the impact of LCZs' spatial arrangement on urban climate and how to optimize the landscape layout for a better thermal environment.

Urban surfaces divided by LCZ classification are described as urban climate landscapes in this paper. They are divided into action landscapes and compensation landscapes according to their mean LST. Action landscapes bring heat load into the city and have higher temperature than urban average level. Others, whose mean temperature is lower, are regarded as compensation landscapes. Landscape-climate interactions and heterogeneities are expressed through urban climate landscape patterns. In this research, we examine the following questions: (1) Can LCZ classification differentiate urban surface temperature effectively? (2) What is the difference in the pattern-temperature relationship across climate landscape types? (3) What metrics impact the thermal effect mostly, and how? By exploring these three questions, we hope to help urban planners to understand the potential impact of climate landscape patterns, so as to optimize urban landscape layout.

2. Materials

2.1. Study Area

Wuhan (29°58′–31°22′N, 113°41′–115°05′E) is one of the largest cities in the central region of China (Figure 1), with a total area of 8569 km^2 and a population of more than 10 million. Located in the east of Jianghan Plain, the Yangtze River runs through the city, and numerous lakes are present within the urban areas. There are four distinct seasons in Wuhan. Summer begins in May and ends in October. It is very hot and humid with abundant rainfall, and the maximum temperature is approximately 37–39 °C. Similar to many developing cities, Wuhan is facing great challenges in urban environment. In this research, the Wuhan metropolitan development area (MDA) is chosen as the study extent, which covers approximately 3268 km^2. With a much higher density of urban construction and urban population, the main urban area (MUA) of the city is used as a comparison extent, which covers 695 km^2.

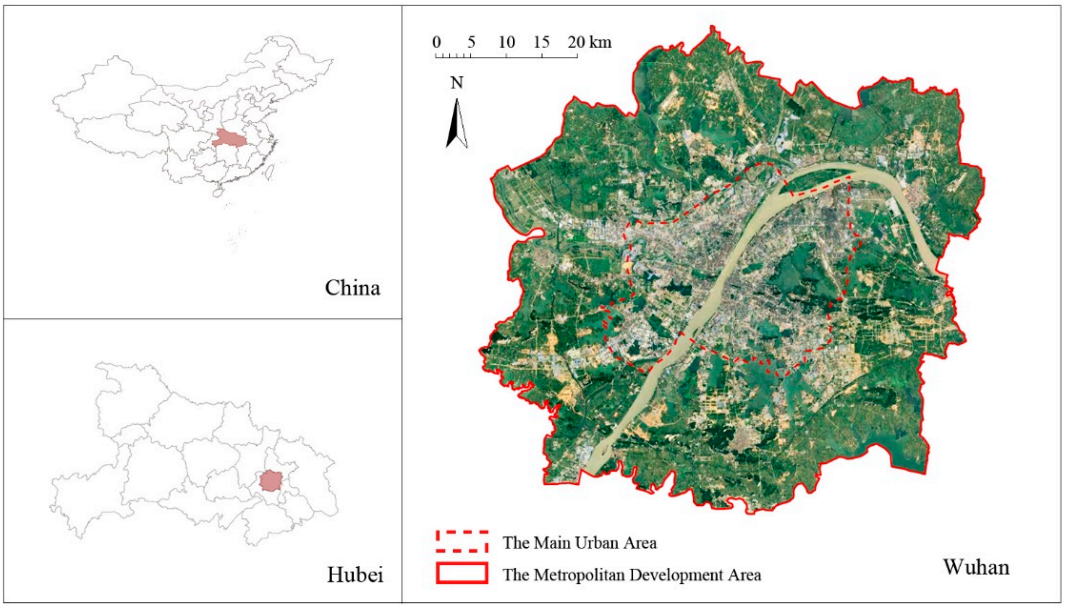

Figure 1. Location map of Wuhan and the study area.

2.2. Data Pre-Processing

Landsat 8 images are employed in this study. Landsat 8 was launched in February 2013, carrying the OLI (Operational Land Imager) and TIRS (Thermal Infrared Sensor). Moderate-resolution imagery is collected from 15 m to 100 m ground cell resolution. Four images taken in spring, summer and fall, respectively, are selected for mapping LCZs. The image data were collected on 26 April, 13 June, 31 July, and 3 October 2013. All these days were calm and cloudless, without rainfall the day before. Data acquired at 10:58 a.m. on 31 July, a typical midsummer day with the maximum temperature of 37 °C, is used to retrieve LST. An extension tool called Landsat 8 LST in ENVI 5.2 SP1 software performed the LST calculation process. The initial resolution of LST raster data is 30 m. Since a 100 m resolution is recommended for LCZ classification (see Section 3.1), LST data are resampled to 100 m.

3. Methodology

We take three steps to achieve the aim of this research: classification; comparison; and quantification. Accordingly, we (1) map LCZs as urban climate landscapes in Wuhan, China; examine the LST differentiation between landscapes; and describe the spatial distribution of urban climate landscapes in order to select focal landscapes; (2) determine the optimal scale to study the pattern-temperature relationship, then compare the relationship between each climate landscape and temperature response; (3) investigate the impact of patch patterns on thermal effect.

3.1. LCZ Classification and Validation

3.1.1. Mapping Local Climate Zones

Among various LCZ classification techniques, the WUDAPT (The World Urban Database and Access Portal Tools) method has the advantages of convenience and versatility [31]. It provides a practical workflow to process the LCZ classification, using open access data and open-source software [32]. Based on the geometry and surface cover properties provided by the LCZ classification framework (Table 1), the urban landscape is observed using Google Earth. Training areas are selected according to land cover types, street aspects, and building spacing requirements specified in local architectural design code. The supervised classification process is performed using SAGA GIS software.

Considering the scale of the LCZ scheme, pattern recognition restrictions, and user requirements [32], an initial resolution of 100 m is adopted. Then, in order to obtain a representative, operable classification map, the optimal patch size of the LCZs is demanded. The initial classification results are filtered using a majority filter, which replaces cells based on the majority of the contiguous neighboring cells. Some research has revealed that 500–650 m is the most suitable scale for accurately characterizing the LST patterns in Wuhan [9]. Therefore, the majority filter radius was set to 3 pixels, that is, the neighboring area covers 5 × 5 cells.

Table 1. Geometric and surface cover properties for local climate zones (LCZs) [23].

LCZ Classes	Sky View Factor	Aspect Ratio	Building Surface Fraction	Impervious Surface Fraction	Pervious Surface Fraction	Height of Roughness Elements
LCZ 1 (Compact Highrise)	0.2–0.4	>2	40–60	40–60	<10	>25
LCZ 2 (Compact Midrise)	0.3–0.6	0.75–2	40–70	30–50	<20	10–25
LCZ 3 (Compact Lowrise)	0.2–0.6	0.75–1.5	40–70	20–50	<30	3–10
LCZ 4 (Open Highrise)	0.5–0.7	0.75–1.25	20–40	30–40	30–40	>25
LCZ 5 (Open Midrise)	0.5–0.8	0.3–0.75	20–40	30–50	20–40	10–25
LCZ 6 (Open Lowrise)	0.6–0.9	0.3–0.75	20–40	20–50	30–60	3–10
LCZ 7 (Lightweight Lowrise)	0.2–0.5	1–2	60–90	<20	<30	2–4
LCZ 8 (Large Lowrise)	>0.7	0.1–0.3	30–50	40–50	<20	3–10
LCZ 9 (Sparsely Built)	>0.8	0.1–0.25	10–20	<20	60–80	3–10
LCZ 10 (Heavy Industry)	0.6–0.9	0.2–0.5	20–30	20–40	40–50	5–15
LCZ A (Dense Trees)	<0.4	>1	<10	<10	>90	3–30
LCZ B (Scattered Trees)	0.5–0.8	0.25–0.75	<10	<10	>90	3–15
LCZ C (Bush, Shrub)	>0.9	0.25–1.0	<10	<10	>90	<2
LCZ D (Low Plants)	>0.9	<0.1	<10	<10	>90	<1
LCZ E (Bare Rock or Paved)	>0.9	<0.1	<10	>90	<10	<0.25
LCZ F (Bare Soil or Sand)	>0.9	<0.1	<10	<10	>90	<0.25
LCZ G (Water)	>0.9	<0.1	<10	<10	>90	-

3.1.2. Validation by LST Variation

The LCZ framework was originally developed to standardize urban temperature observations [23]. Air temperatures of each zones are significantly difference [33]. Because of the close relationship between LST and air temperature [34], we assume that the LSTs of each zone should also be significantly different. Thus the assumption is that the LCZ classification is determined by the land surface characteristics, which in turn affects the zonal patterns of the LST. In this case, analysis of variance (ANOVA) is used to examine the ability of the LCZs to differentiate LSTs across climate landscapes. Tamhane's T2 post hoc is used to investigate the differences between each pair of LCZs.

3.2. Comparison of Different Landscapes

3.2.1. Urban Climate Landscape Pattern

A series of landscape metrics are used for quantifying the spatial distribution of climate landscapes, which are computed using the Fragstats 4.2.1 software package [35]. Three aspects are often considered in urban planning, namely, area, shape geometry, and relationship with other landscapes. All metrics selected in this study revolve around these factors (Table 2). In this research, spatial characteristics of individual patches are quantified by patch level metrics, general character of each climate landscape type by class level metrics; and overall landscape pattern of the given extent by landscape level metrics.

3.2.2. Searching for the Optimal Scale

Attention should be paid to spatial scale or resolution when analyzing remote sensing imagery [8,36]. Since landscape patterns and their relationships tend to vary at different observational scales [37], the optimal scale is required for the examination. The moving window method is applied to calculate continuous landscape metrics. For each pixel, seven window sizes are tested (300 m,

500 m, 700 m, 900 m, 1100 m, 1300 m, and 1500 m). The patch pattern is measured by three landscape metrics (Table 2) including area-weighted mean perimeter-area ratio (PARA_AM), Shannon's diversity index (SHDI), and total edge contrast index (TECI). Pearson's correlation coefficients between metric values from seven window sizes and LSTs of the center points were examined to search for the optimal window size.

Table 2. Descriptions of landscape metrics used in this study [35].

Abbreviation	Landscape Metrics	Description	Analysis Level
AREA	Area	The area of the patch.	Patch level
SHAPE	Shape Index	The simplest and straightforward measure of shape complexity.	Patch level
CAI	Core Area Index	A relative index that quantifies core area as a percentage of patch area.	Patch level
ECON	Edge Contrast Index	A relative measure of the amount of contrast along the patch perimeter.	Patch level
PLAND	Percentage of Landscape	The percentage the landscape comprised of the corresponding patch type.	Class level
PARA_AM	Area-Weighted Mean Perimeter-Area Ratio	PARA is a simple measure of shape complexity.	Landscape level
SHDI	Shannon's Diversity Index	A popular measure of diversity in community ecology.	Landscape level
TECI	Total Edge Contrast Index	A relative measure of the amount of contrast along the patch perimeter.	Landscape level
PD	Patch Density	The number of patches on a per unit area basis.	Landscape level
AREA_MN	Mean Patch Area	Average patch area of the landscape.	Landscape level
TCA	Total Core Area	The sum of the core areas of each patch of the landscape.	Landscape level

3.2.3. Comparison of the Pattern-Temperature Relationship

The pattern-temperature relationship of each landscape is investigated by randomly sampled pixels. First, a total of 100 pixels in each landscape are selected randomly. Taking every pixel as a center, we buffer a square area at the optimal scale to observe the surrounding landscape patterns. Then, six metrics are computed to describe the composition and construction of landscapes (Table 2), including patch density (PD), mean patch area (AREA_MN), total core area (TCA), as well as PARA_AM, TECI, and SHDI. At last, the pixel LST and maximum/minimum LST in the buffer area are correlated with landscape metrics to uncover any relationships.

3.3. Quantification of the Heating/Cooling Effect

3.3.1. Defining the Heating/Cooling Intensity

The thermal effects on the surrounding environment by climate landscape patches are considered as heating intensity for action landscapes and cooling intensity for compensation landscapes. In this paper, heating intensity = $LST_{patch\_max} - LST_{mean}$; cooling intensity = $LST_{patch\_min} - LST_{mean}$, where LST_{patch_max} is the maximum LST of the patch, LST_{patch_min} is the minimal LST of the patch, and LST_{mean} is the mean LST of the whole study area.

3.3.2. Quantifying the Effect by Patch Metrics

To estimate the contribution of patch metrics to heating/cooling effect, four landscape metrics are selected to represent landscape pattern characteristics at the patch level (Table 2). They are area (AREA), shape index (SHAPE), core area index (CAI), and edge contrast index (ECON). Core area is

defined as the area of the patch 100 m away from the edge; the edge contrast is determined by the temperature difference between the average LSTs of each class. A step-wise multivariate regression is used to evaluate the roles of climate landscape patterns on heating and cooling intensity at the patch level.

4. Results and Discussion

4.1. LCZ Map of Wuhan

The LCZ classification results in Wuhan are shown in Figure 2. There are 17 classes within the initial LCZ framework (Table 1). Based on four Landsat 8 images from 2013, 16 classes are present due to the lack of a Lightweight Lowrise class. Different radii (from 1 to 5 pixels) of the majority filter are applied respectively to the classification result. As the radius increases, fragmented pixels are removed (Figure 2a,b), and gradually, more detail is lost (Figure 2d,e). Considering the readability of the classification result, the applicability of the LCZs to the urban planning process, and the operational scale of the LST dynamic in Wuhan [9], Figure 2c is selected for analysis.

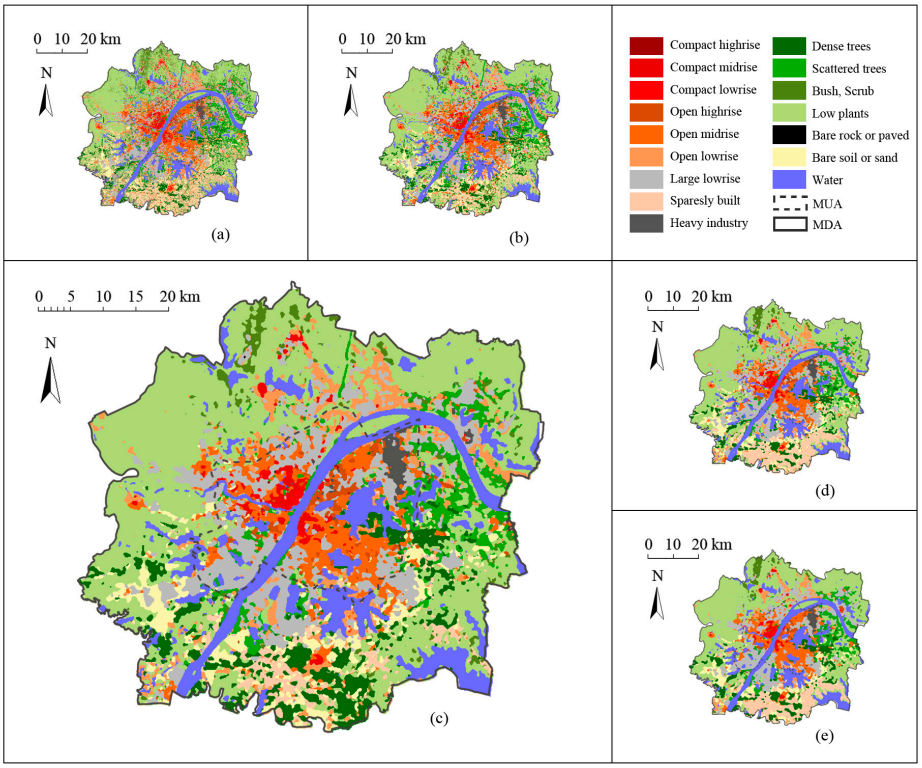

Figure 2. LCZ maps of Wuhan applied with a majority filter. The radius is (**a**) 1 pixel, (**b**) 2 pixels, (**c**) 3 pixels, (**d**) 4 pixels, (**e**) 5 pixels.

4.2. Verifying LCZs by LST Variation

4.2.1. Distribution of LST

As shown in Figure 3, the LST distribution in Wuhan is uneven. The urban built-up environment is warmer than other areas (Figure 3). The average LST of the MDA is 35.66 °C and the standard deviation is 4.45 °C (Figure 4). Comparatively, the average LST of the MUA is 3.13 °C higher than the MDA, reaching 38.79 °C with a standard deviation of 5.00 °C. The core area of the city is significantly overheated.

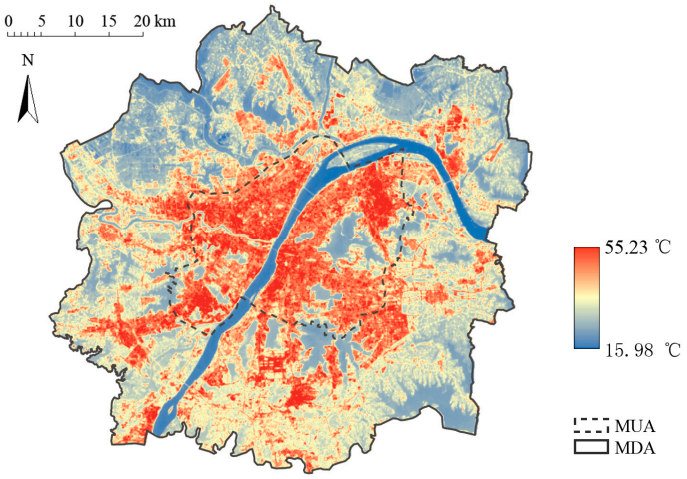

Figure 3. Land surface temperature (LST) map retrieved from Landsat 8 imagery on 31 July 2013.

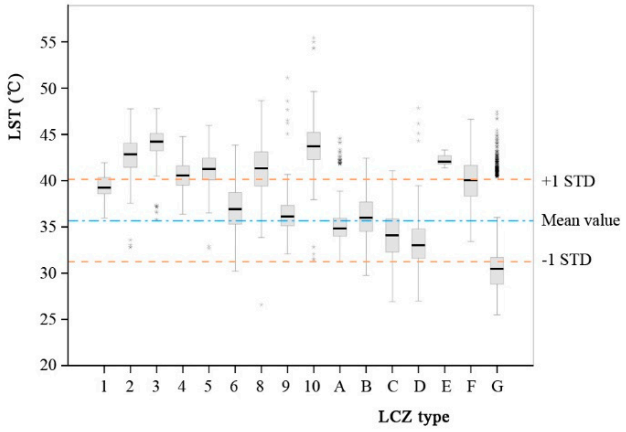

Figure 4. Boxplot of LST distribution.

Figure 4 shows the LST distribution of all climate landscapes. Action landscapes include the built-up environment and bare land. Excessively high temperature is present in the Compact Lowrise (mean LST is 44.01 °C) and the Heavy Industry landscape (mean LST is 43.83 °C). The Compact Midrise and Bare Rock landscapes also show elevated heat levels. Vegetation and waterbody areas belong to compensation landscapes, which play the role of balancing and lowering temperature. Other landscapes, such as Open Lowrise, Sparsely Built, Dense Trees, Scattered Trees, are moderate in this case.

4.2.2. Validation of LCZ Classification

Due to differences in urban morphology and artificial heat emission, air temperature readings vary across each LCZ class [33]. In this study, the results of ANOVA show that there is also a significant difference between the mean LSTs in all 16 classes, and the significance level is 0.000. Furthermore, the results of Tamhane's T2 post hoc show a significant difference between the average LSTs of most of the 120 pairs for all 16 classes (Table 3). At the 0.05 confidence level, only four pairs, that is, Compact Highrise and Bare Soil or Sand, Compact Midrise and Bare Rock or Paved, Compact Lowrise and Heavy Industry, and Open Midrise and Large Lowrise, exhibit an insignificant difference. Open Midrise and Bare Rock or Paved is included at the 0.01 confidence level. This indicates that the LCZ classification result is considered to be acceptable for this preliminary study.

Table 3. Tamhane's T2 multiple comparison table of mean differences in LST of LCZ classes.

	LCZ 1	**LCZ 2**	**LCZ 3**	**LCZ 4**	**LCZ 5**	**LCZ 6**	**LCZ 8**	**LCZ 9**	**LCZ 10**	**LCZ A**	**LCZ B**	**LCZ C**	**LCZ D**	**LCZ E**	**LCZ F**
LCZ 2	−3.212 *														
LCZ 3	−4.671 *	−1.459 *													
LCZ 4	−1.187 *	2.025 *	3.484 *												
LCZ 5	−1.831 *	1.382 *	2.841 *	−0.644 *											
LCZ 6	2.184 *	5.397 *	6.856 *	3.371 *	4.015 *										
LCZ 8	−1.837 *	1.376 *	2.835 *	−0.649 *	−0.006	−4.021 *									
LCZ 9	3.037 *	6.249 *	7.708 *	4.224 *	4.868 *	0.853 *	4.873 *								
LCZ 10	−4.493 *	−1.280 *	0.179	−3.305 *	−2.662 *	−6.677 *	−2.656 *	−7.529 *							
LCZ A	4.228 *	7.441 *	8.900 *	5.415 *	6.059 *	2.044 *	6.065 *	1.192 *	8.721 *						
LCZ B	3.238 *	6.451 *	7.910 *	4.425 *	5.069 *	1.054 *	5.075 *	0.201 *	7.731 *	−0.990 *					
LCZ C	5.284 *	8.496 *	9.955 *	6.471 *	7.114 *	3.099 *	7.120 *	2.247 *	9.776 *	1.055 *	2.046 *				
LCZ D	6.014 *	9.226 *	10.685 *	7.201 *	7.845 *	3.830 *	7.851 *	2.977 *	10.507 *	1.786 *	2.776 *	0.730 *			
LCZ E	−2.936 *	0.277	1.736 *	−1.749 *	−1.105 *	−5.120 *	−1.099 *	−5.973 *	1.557 *	−7.164 *	−6.174 *	−8.219 *	−8.950 *		
LCZ F	−0.625	2.588 *	4.046 *	0.562 *	1.206 *	−2.809 *	1.212 *	−3.662 *	3.868 *	−4.853 *	−3.863 *	−5.909 *	−6.639 *	2.311 *	
LCZ G	8.749 *	11.961 *	13.420 *	9.936 *	10.580 *	6.565 *	10.585 *	5.712 *	13.241 *	4.521 *	5.511 *	3.465 *	2.735 *	11.685 *	9.374 *

* The mean difference is significant at the 0.05 level (2-tailed).

4.3. Spatial Distribution of Urban Climate Landscape and Focal Landscapes

4.3.1. Area Proportion of Each Climate Landscape

Figure 5 shows the proportion of each climate landscape area, that is, percentage of landscape (PLAND). Low Plants occupies the largest area in the MDA, but it is much less in the MUA. Areas of Large Lowrise and Open Midrise account for the largest proportion in the MUA. With larger area proportions in the MUA than in the MDA, most built-up landscapes are concentrated in the core area of the city, and are surrounded by a large number of agricultural landscapes. The total proportion of vegetation in MUA is less than 12%. Due to the lack of vegetation, water is the most important compensation landscape in Wuhan. It is noteworthy that the area proportion of Water in the MUA is 19.7%, which is greater than the proportion of Water in the MDA.

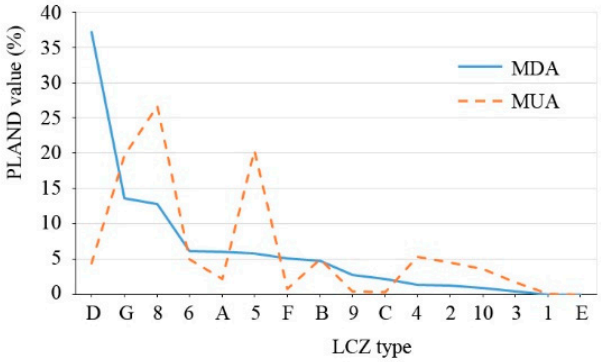

Figure 5. Proportion of each climate landscape area, sorted by PLAND values in the metropolitan development area (MDA).

4.3.2. Selection of Focal Climate Landscapes

Not all climate landscapes have the same impact on urban thermal environment. Some deserve more attention than others. Based on the area, distribution, and temperature, three criteria are established to screen focal climate landscapes in this case study. First, the number of samples must be sufficient in order to ensure the validity of the analysis results. Areas with a PLAND less than 0.1% are disregarded. Second, the spatial distribution should be concentrated to the MUA, which indicates that the core area of the city needs more attention. Areas with larger PLAND in the MUA than in the MDA are considered to satisfy this criterion. Third, the LCZ should show a significant temperature difference, and the average LST must be beyond ± 1 standard deviation from the mean LST of the whole study area (Figure 4).

Table 4 shows whether each landscape meets these three criteria. As a result, Compact Midrise, Compact Lowrise, Open Highrise, Open Midrise, Large Lowrise, Heavy Industry, and Water are selected as focal landscapes for further analysis.

4.4. Optimal Scale for Studying Pattern-Temperature Interactions

A moving window analysis is applied to examine the correlation between landscape patterns and LSTs at seven spatial scales (from 300 m to 1500 m, at 200 m intervals). Pearson correlation coefficients of each window size are plotted in Figure 6. For most focal landscapes, PARA_AM and TECI show the strongest correlation with LST at the 300–700 m scale, and SHDI shows the strongest correlation with LST at the 500–700 m scale. For the Water landscape, the correlation between SHDI and LST reaches a maximum of 0.585 at the 700 m scale, which is close to 0.580 at the 500 m scale. This implies that the 500 m scale is a good choice to study pattern-temperature interactions in Wuhan, since most of the interactions show highest correlativity at this scale. The scale effect of the Heavy Industry landscape is

peculiar, and PARA_AM and SHDI correlate best with LST at 1300 m and 1500 m, respectively. This may be due to high-intensity artificial heat sources which is distinct from all other landscapes.

Table 4. Selection of focal climate landscapes.

	Sufficient Area	Centralized Distribution	Adequate Temperature Difference
LCZ 1 (Compact Highrise)	-	√	-
LCZ 2 (Compact Midrise)	√	√	√
LCZ 3 (Compact Lowrise)	√	√	√
LCZ 4 (Open Highrise)	√	√	√
LCZ 5 (Open Midrise)	√	√	√
LCZ 6 (Open Lowrise)	√	-	-
LCZ 8 (Large Lowrise)	√	√	√
LCZ 9 (Sparsely Built)	√	-	-
LCZ 10 (Heavy Industry)	√	√	√
LCZ A (Dense Trees)	√	-	-
LCZ B (Scattered Trees)	√	-	-
LCZ C (Bush, Shrub)	√	-	-
LCZ D (Low Plants)	√	-	-
LCZ E (Bare Rock or Paved)	-	√	√
LCZ F (Bare Soil or Sand)	√	-	-
LCZ G (Water)	√	√	√

Note: The landscapes that meet all criteria are highlighted.

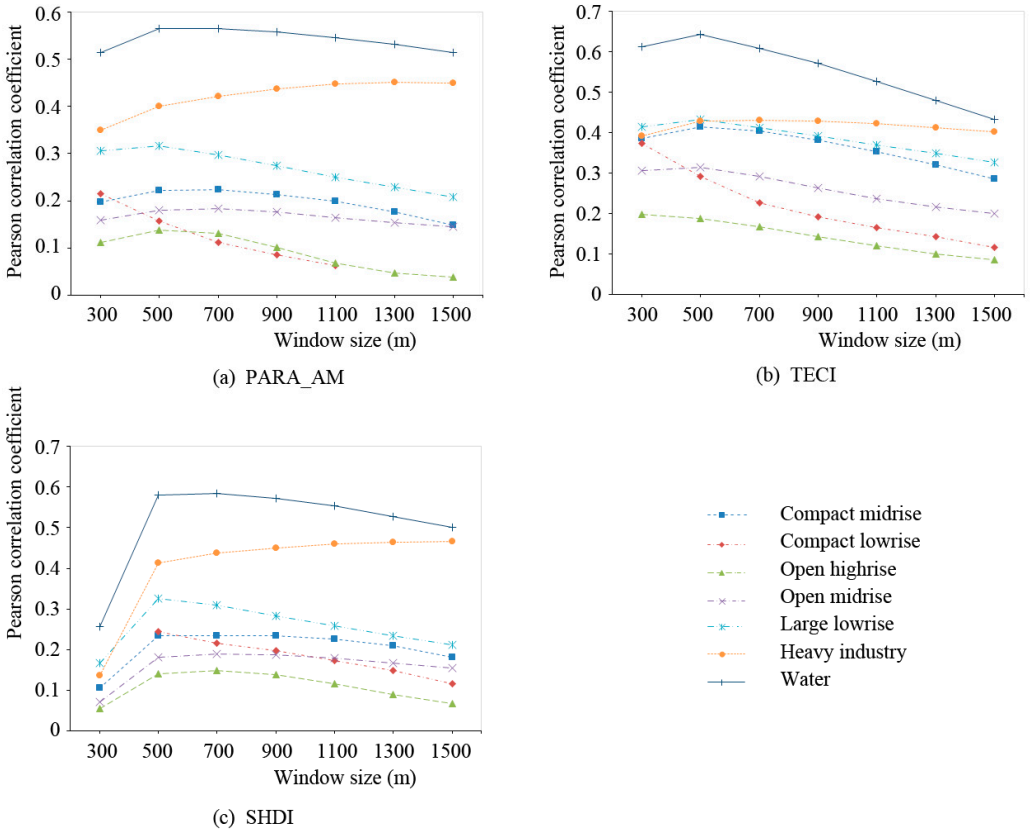

Figure 6. Pearson correlation coefficient between landscape metrics and LST in different window sizes: (**a**) PARA_AM; (**b**) TECI; (**c**) SHDI.

Since both landscape patterns and LST distributions are scale dependent, it is important to examine the scale effects in a specific case study before investigating the interrelationships. According to previous studies, the optimal research scale in urban area varies, for example, from 120 m in Indianapolis, USA [38], to 660–720 m in Beijing, China [8]. A case study in Wuhan suggests that the appropriate scale to inspect the LST and its cause is 500–650 m [9]. This is consistent with our optimal scale and verifies that 500 m is a suitable scale to investigate landscape-climate interactions locally.

4.5. Relationship between Landscape Metrics and LST at a Fixed Scale

Given the 500 m window size, the influence of landscape patterns on temperature varies (Figure 7). Among these metrics, TECI, which represents the temperature difference between adjacent patches, has the most stable effect on LST, negatively for action landscapes and positively for compensation landscape. Noticeably, patch temperature is affected by adjacent patches. For all action landscapes, LST negatively correlates with PD, PARA_AM, and SHDI, and positively correlates with AREA_MN and TCA. This result demonstrates the benefit of a fragmental landscape pattern, that is, patches with small area, large density and complex shape. For the compensation landscape, the situation is reversed. Generally, fragmental landscape patches and large edge contrast of temperature contribute to heat release.

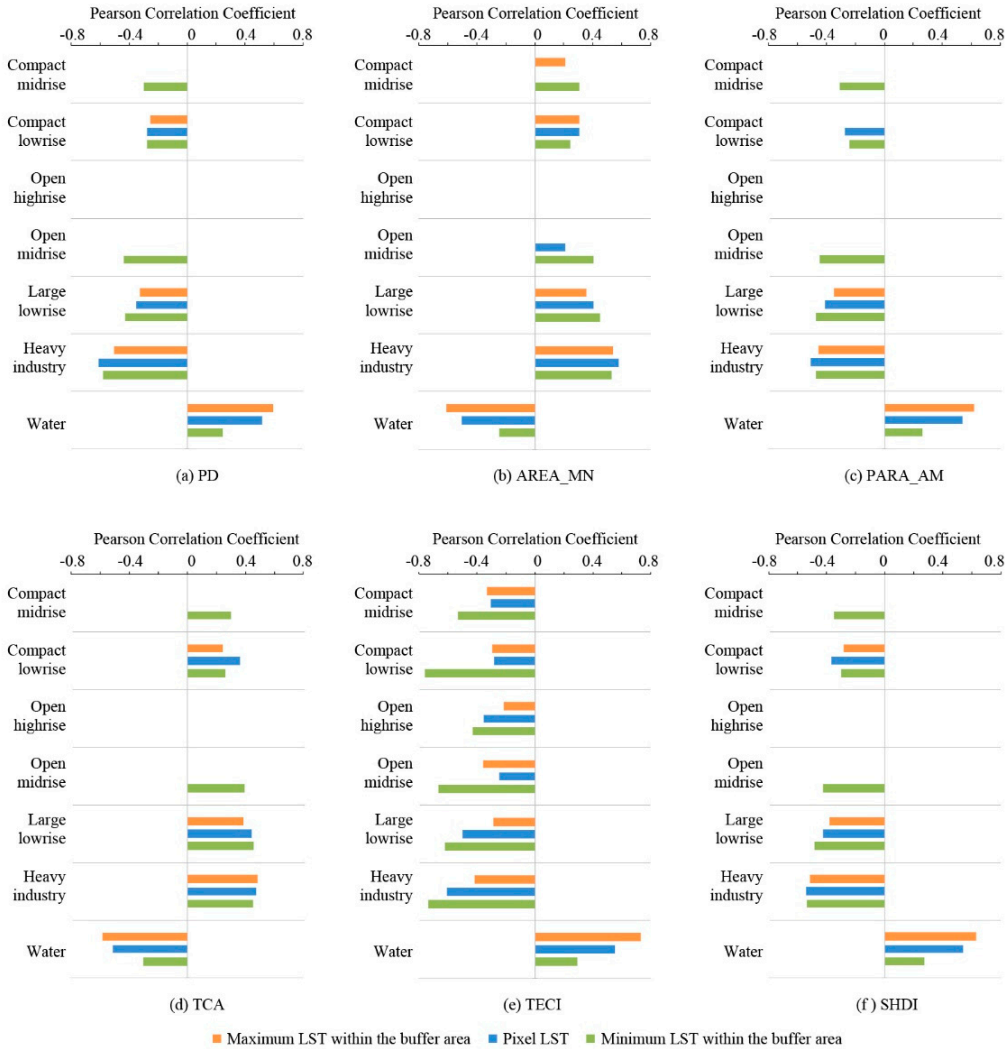

Figure 7. Comparison of Pearson correlation coefficients between landscape metrics and LSTs: (**a**) PD; (**b**) AREA_MN; (**c**) PARA_AM; (**d**) TCA; (**e**) TECI; (**f**) SHDI.

For those landscapes whose mean LST deviates far from the mean LST of the whole city (Figure 4), such as Compact Lowrise, Large Lowrise, Heavy Industry, and Water, landscape metrics have greater influence on pixel LSTs. And moderate ones are less impacted by landscape patterns. In other words, layout optimization will be more effective in those landscapes with extreme temperatures, thus priority should be given to those types in planning decision process.

In the case of action landscapes, the effect of pattern characteristics on minimum LST is stronger than that on maximum LST, especially for the Compact Midrise, Open Midrise, and Large Lowrise landscapes. That is to say, the minimum LST of action landscapes is more affected by landscape patterns, while the maximum LST is relatively stable. Specific surface characteristics and artificial heat release cause increasing temperature, while reasonable landscape patterns contribute to decreasing temperature. For compensation landscapes, this relationship is reversed.

Some results of specific landscapes are worth noting. For the Open Highrise landscape, TECI is the only metric to show any visible correlation with temperature. Compared with other landscape types, the Open Highrise landscape is hardly affected by landscape pattern. Low density, high buildings, and adequate vegetation result in better ventilation and lower temperature [39]. This finding implies that flexible layout of the highrise landscape is acceptable because it does not impact local climate significantly.

The LSTs of the Heavy Industry landscape correlate well with landscape pattern with a correlation coefficient greater than 0.5. Despite excessive heat stress, the thermal environment of the Heavy Industry landscape may be effectively mitigated by optimizing the landscape pattern. Reducing the patch area, increasing patch shape complexity, and bordering compensation space are effective methods of landscape optimization.

The Compact Lowrise landscape, which has the highest mean LST among all landscapes, is generally similar to other action landscapes, but more complex. Landscape pattern and LSTs show a moderate correlation with an irregular variation. This may be due to the complicated land surface composition, low vegetation, and a large percentage of impervious surfaces [10,12]. Particularly, TECI shows a strong correlation with the minimum LST ($r = 0.758$). This shows that controlling the patch area, as well as adjoining to compensation landscapes, is essential.

4.6. Impact of Patch Metrics on LST

Table 5 shows the results of the step-wise multivariate regression. The coefficients of determination (R2) measures the proportion of the variance in heating/cooling intensity that is predictable from the patch metric(s). The standardized coefficients tell us which metric has a greater impact on patch heating/cooling intensity in the regression model. Tolerance and VIF examine the collinearity of the predictor variables.

For Compact Midrise, Open Highrise, Open Midrise, and Large Lowrise landscapes, patch heating intensity is affected by ECON, CAI, and SHAPE. When these three metrics are included as predictor variables, the model accounts for 53.3% of the heating intensity variance for the Large Lowrise landscape, and CAI has the greatest impact on patch heating intensity. For Compact Midrise and Open Midrise landscapes, the predictable proportion is 51.2% and 49.0%, and the most effective predictor variables are ECON and CAI respectively. So it can be inferred that for these types of landscapes, it is worth paying special attention to patch geometry in the planning process, especially the core area of the patch and the temperature difference between adjacent patches.

Given extreme heat stress, patch heating intensity of Heavy Industry is less affected by patch metrics. Only 26.8% can be explained by the shape complexity index. Since the influence of patch geometry is limited, mitigation strategies integrating the surrounding environment should be considered for the Heavy Industry landscape.

Table 5. Regression results with landscape metrics as independent variables and heating/cooling intensity as dependent variable.

		Model	Unstandardized Coefficients		Standardized Coefficients	*t*	Sig.	Collinearity Statistics		Adjusted R Square
			B	Std. Error	Beta			Tolerance	VIF	
Heating intensity	LCZ 2 (Compact Midrise)	(Constant)	7.117	0.938		7.587	0.000			0.512
		ECON	−0.102	0.015	−0.495	−6.574	0.000	0.958	1.044	
		CAI	0.030	0.010	0.261	3.126	0.002	0.775	1.290	
		SHAPE	2.005	0.663	0.255	3.024	0.003	0.765	1.307	
	LCZ 3 (Compact Lowrise)	(Constant)	8.701	0.262		33.185	0.000			0.347
		CAI	0.049	0.009	0.599	5.599	0.000	1.000	1.000	
	LCZ 4 (Open Highrise)	(Constant)	4.178	0.680		6.141	0.000			0.353
		CAI	0.045	0.007	0.462	6.053	0.000	0.689	1.452	
		ECON	−0.033	0.013	−0.167	−2.593	0.010	0.969	1.032	
		SHAPE	1.371	0.602	0.174	2.279	0.024	0.687	1.456	
	LCZ 5 (Open Midrise)	(Constant)	5.798	0.393		14.747	0.000			0.490
		CAI	0.057	0.005	0.507	10.693	0.000	0.983	1.017	
		ECON	−0.066	0.009	−0.306	−7.411	0.000	0.742	1.348	
		SHAPE	0.884	0.274	0.152	3.226	0.001	0.752	1.329	
	LCZ 8 (Large Lowrise)	(Constant)	6.327	0.499		12.684	0.000			0.533
		CAI	0.068	0.006	0.512	11.770	0.000	0.995	1.005	
		ECON	−0.091	0.010	−0.347	−9.592	0.000	0.687	1.456	
		SHAPE	1.336	0.333	0.175	4.018	0.000	0.685	1.459	
	LCZ 10 (Heavy Industry)	(Constant)	0.755	1.835		0.412	0.682			0.268
		SHAPE	6.452	1.470	0.531	4.389	0.000	1.000	1.000	
Cooling intensity	LCZ G (Water)	(Constant)	−5.020	0.360		−13.932	0.000			0.574
		CAI	−0.034	0.004	−0.399	−7.696	0.000	0.988	1.012	
		AREA	−0.001	0.000	−0.396	−7.681	0.000	0.694	1.441	
		ECON	0.056	0.007	0.372	7.627	0.000	0.701	1.427	

Previous researchers report that similar to vegetation, urban waterbodies can reduce the temperature of the ambient environment [40], and waterbody geometry significantly influences cooling capacity [41]. Consistently, our regression result shows that patch cooling intensity of Water is affected by CAI, AREA, and ECON, and 57.4% of cooling intensity variation can be explained by the regression model (Table 5). These three metrics have almost equal effects on the cooling intensity. This means that the area, especially the core area, is the main factor impacting waterbody cooling intensity. But in many cities, water area is continuously shrinking during the process of urban renewal and urbanization. To ensure the cooling effect, maintaining waterbody area plays a vital role in tackling urban overheating and should be a fundamental measure.

5. Implications and Conclusions

The global concern on climate change highlights the need for urban planning [42]. However, due to the difficulty of understanding complex climate variations within cities and the lack of consideration of climate knowledge in local urban planning practices, climate actions adopted by urban planners are still limited and ineffective [1,43]. Although knowledge is not easily transferable from climate science to urban planning [44], LCZ classification presents an opportunity to bridge the gap between research and practice. It classifies land surfaces according to climate related urban morphology [23] so as to examine the diversity and complexity of the climate response within a city. From the perspective of urban planners, urban surfaces classified by LCZ are regarded as urban climate landscapes in this paper.

Urban climate landscapes provide a much-needed climate perspective to understand urban landscapes and extend the concept of LCZ to urban planning applications. Climate-related classification results at the local scale effectively distinguish climate diversity and are easily applied to urban planning because of the land-based zoning strategy. For specific locations, classification results present the climatic response of urban surface, which can provide comparison and guiding urban

planning [45]. Through the lens of urban climate landscapes, past and future local climate studies can be examined to provide an overall climate picture of the city.

Land cover conditions impact UHIs at the metropolitan scale [46]. Similarly, analysis of the pattern-temperature relationship in this study shows the climate effects of land-use patterns at the local scale. In fact, the impact of landscape layout on urban thermal environment has been seldom considered in conventional urban planning regulation. This research reveals the effective landscape metrics and their impacts on different landscape types. These results can provide guidance in the urban planning process. For example, when planners consider the climate landscape layout, attention should be paid to urban climate landscape configuration, and land-based planning strategies, including large temperature contrasts between adjacent patches, and fragmental patches, are recommended. These strategies should be taken into account in the early stage of land-use planning, or be used as guidance in the urban renewal process. Combining with other adaptation approaches, such as urban reforestation and green roofs, a reasonable climate landscape layout will benefit to mitigate overheating.

At present, a growing subset of research explores the urban thermal environment based on LCZ in urban areas. Since every city is unique, local knowledge, such as land surface characteristics, topographic features and cultural backgrounds, should be considered in the classification process, and the optimal scale analysis is necessary. However, the methodology adopted in this study is general, and the conclusions drawn from this case study also provide reference for subtropical developing cities. In this case study, focal landscapes are examined, and the local optimal scale is identified. It is instructive to subdivide and quantify particular landscapes in further research, such as the complex Compact Lowrise and the hot Heavy Industry in Wuhan. High spatial and temporal resolution data may also improve the accuracy of LCZ classification in future research. Highlighting the impact of urban climate landscape patterns, our study acts as a basis for future examinations of urban climate for landscape planners and urban designers.

Acknowledgments: This work was supported by the National Natural Science Foundation of China [No. 51378399]; and [No. 41331175].

Author Contributions: Qingming Zhan guided this study, developed the research framework, and revised the manuscript; Yasha Wang conducted the case study, performed the data analysis, and wrote the initial daft of this paper; Wanlu Ouyang prepared the data, provide the basic process of calculation, and contributed to revise the manuscript.

Conflicts of Interest: The authors declare no conflict of interest.

References

1. Hoag, H. How cities can beat the heat: Rising temperatures are threatening urban areas, but efforts to cool them may not work as planned. *Nature* **2015**, *524*, 402–405. [CrossRef] [PubMed]
2. IPCC. *Climate Change 2014: Synthesis Report. Contribution of Working Groups I, II and III to the Fifth Assessment Report of the Intergovernmental Panel on Climate Change*; IPCC: Cambridge, UK, 2014.
3. Grimmond, C.S.B.; Roth, M.; Oke, T.R.; Au, Y.C.; Best, M.; Betts, R.; Carmichael, G.; Cleugh, H.; Dabberdt, W.; Emmanuel, R. Climate and more sustainable cities: Climate information for improved planning and management of cities. *Procedia Environ. Sci.* **2010**, *1*, 247–274. [CrossRef]
4. Adolphe, L. A simplified model of urban morphology: Application to an analysis of the environmental performance of cities. *Environ. Plan. B Plan. Des.* **2001**, *28*, 183–200. [CrossRef]
5. Unger, J. Intra-urban relationship between surface geometry and urban heat island: Review and new approach. *Clim. Res.* **2004**, *27*, 253–264. [CrossRef]
6. Zhao, C.; Fu, G.; Liu, X.; Fu, F. Urban planning indicators, morphology and climate indicators: A case study for a north-south transect of beijing, China. *Build. Environ.* **2011**, *46*, 1174–1183. [CrossRef]
7. Voogt, J.A.; Oke, T.R. Thermal remote sensing of urban climates. *Remote Sens. Environ.* **2003**, *86*, 370–384. [CrossRef]
8. Song, J.; Du, S.; Feng, X.; Guo, L. The relationships between landscape compositions and land surface temperature: Quantifying their resolution sensitivity with spatial regression models. *Landsc. Urban Plan.* **2014**, *123*, 145–157. [CrossRef]

9. Wang, J.; Zhan, Q.; Guo, H.; Jin, Z. Characterizing the spatial dynamics of land surface temperature-impervious surface fraction relationship. *Int. J. Appl. Earth Obs. Geoinf.* **2016**, *45*, 55–65. [CrossRef]
10. Myint, S.W.; Zheng, B.; Talen, E.; Fan, C.; Kaplan, S.; Middel, A.; Smith, M.; Huang, H.P.; Brazel, A. Does the spatial arrangement of urban landscape matter? Examples of urban warming and cooling in phoenix and las vegas. *Ecosyst. Health Sustain.* **2015**, *1*, 15.
11. Cao, X.; Onishi, A.; Chen, J.; Imura, H. Quantifying the cool island intensity of urban parks using aster and ikonos data. *Landsc. Urban Plan.* **2010**, *96*, 224–231. [CrossRef]
12. Li, J.; Song, C.; Cao, L.; Zhu, F.; Meng, X.; Wu, J. Impacts of landscape structure on surface urban heat islands: A case study of shanghai, china. *Remote Sens. Environ.* **2011**, *115*, 3249–3263. [CrossRef]
13. Kong, F.; Yin, H.; Wang, C.; Cavan, G.; James, P. A satellite image-based analysis of factors contributing to the green-space cool island intensity on a city scale. *Urban Green.* **2014**, *13*, 846–853. [CrossRef]
14. Feng, X.; Myint, S.W. Exploring the effect of neighboring land cover pattern on land surface temperature of central building objects. *Build. Environ.* **2016**, *95*, 346–354. [CrossRef]
15. Matthews, T.; Lo, A.Y.; Byrne, J.A. Reconceptualizing green infrastructure for climate change adaptation: Barriers to adoption and drivers for uptake by spatial planners. *Landsc. Urban Plan.* **2015**, *138*, 155–163. [CrossRef]
16. Emmanuel, R.; Loconsole, A. Green infrastructure as an adaptation approach to tackling urban overheating in the glasgow clyde valley region, UK. *Landsc. Urban Plan.* **2015**, *138*, 71–86. [CrossRef]
17. Jim, C.Y.; Chan, M.W.H. Urban greenspace delivery in hong kong: Spatial-institutional limitations and solutions. *Urban Green.* **2016**, *18*, 65–85. [CrossRef]
18. Demuzere, M.; Orru, K.; Heidrich, O.; Olazabal, E.; Geneletti, D.; Orru, H.; Bhave, A.; Mittal, N.; Feliu, E.; Faehnle, M. Mitigating and adapting to climate change: Multi-functional and multi-scale assessment of green urban infrastructure. *J. Environ. Manag.* **2014**, *146*, 107–115. [CrossRef] [PubMed]
19. Yuan, C.; Ng, E. Building porosity for better urban ventilation in high-density cities—A computational parametric study. *Build. Environ.* **2012**, *50*, 176–189. [CrossRef]
20. Gál, T.; Unger, J. Detection of ventilation paths using high-resolution roughness parameter mapping in a large urban area. *Build. Environ.* **2009**, *44*, 198–206. [CrossRef]
21. Karlessi, T.; Santamouris, M.; Synnefa, A.; Assimakopoulos, D.; Didaskalopoulos, P.; Apostolakis, K. Development and testing of pcm doped cool colored coatings to mitigate urban heat island and cool buildings. *Build. Environ.* **2011**, *46*, 570–576. [CrossRef]
22. Larsen, L. Urban climate and adaptation strategies. *Front. Ecol. Environ.* **2015**, *13*, 486–492. [CrossRef]
23. Stewart, I.D.; Oke, T.R. Local climate zones for urban temperature studies. *Bull. Am. Meteorol. Soc.* **2012**, *93*, 1879–1900. [CrossRef]
24. Wang, J.; Ouyang, W. Attenuating the surface urban heat island within the local thermal zones through land surface modification. *J. Environ. Manag.* **2017**, *187*, 239–252. [CrossRef] [PubMed]
25. Geletič, J.; Lehnert, M.; Dobrovolný, P. Land surface temperature differences within local climate zones, based on two central european cities. *Remote Sens.* **2016**, *8*, 788. [CrossRef]
26. Bechtel, B.; See, L.; Mills, G.; Foley, M. Classification of local climate zones using sar and multispectral data in an arid environment. *IEEE J. Sel. Top. Appl. Earth Obs. Remote Sens.* **2016**, *9*, 3097–3105. [CrossRef]
27. Danylo, O.; See, L.; Bechtel, B.; Schepaschenko, D.; Fritz, S. Contributing to wudapt: A local climate zone classification of two cities in ukraine. *IEEE J. Sel. Top. Appl. Earth Obs. Remote Sens.* **2016**, *9*, 1841–1853. [CrossRef]
28. Xu, Y.; Ren, C.; Cai, M.; Edward, N.Y.Y.; Wu, T. Classification of local climate zones using aster and landsat data for high-density cities. *IEEE J. Sel. Top. Appl. Earth Obs. Remote Sens.* **2017**, *10*, 3397–3405. [CrossRef]
29. Leconte, F.; Bouyer, J.; Claverie, R.; Pétrissans, M. Using local climate zone scheme for UHI assessment: Evaluation of the method using mobile measurements. *Build. Environ.* **2015**, *83*, 39–49. [CrossRef]
30. Middel, A.; Häb, K.; Brazel, A.J.; Martin, C.A.; Guhathakurta, S. Impact of urban form and design on mid-afternoon microclimate in phoenix local climate zones. *Landsc. Urban Plan.* **2014**, *122*, 16–28. [CrossRef]
31. Mills, G.; Ching, J.; See, L.; Bechtel, B.; Foley, M. An introduction to the wudapt project. In Proceedings of the 9th International Conference on Urban Climate, Toulouse, France, 20–24 July 2015; pp. 20–24.

32. Bechtel, B.; Alexander, P.J.; Böhner, J.; Ching, J.; Conrad, O.; Feddema, J.; Mills, G.; See, L.; Stewart, I.D. Mapping local climate zones for a worldwide database of the form and function of cities. *ISPRS Int. J. Geo-Inf.* **2015**, *4*, 199–219. [CrossRef]
33. Stewart, I.D.; Oke, T.R.; Krayenhoff, E.S. Evaluation of the 'local climate zone' scheme using temperature observations and model simulations. *Int. J. Climatol.* **2014**, *34*, 1062–1080. [CrossRef]
34. Schwarz, N.; Schlink, U.; Franck, U.; Großmann, K. Relationship of land surface and air temperatures and its implications for quantifying urban heat island indicators—An application for the city of leipzig. *Ecol. Indic.* **2012**, *18*, 693–704. [CrossRef]
35. McGarigal, K.; Cushman, S.A.; Ene, E. Spatial Pattern Analysis Program for Categorical and Continuous Maps. Available online: http://www.umass.edu/landeco/research/fragstats/fragstats.html (accessed on 20 September 2017).
36. Goodchild, M.F.; Quattrochi, D.A. Scale, Multiscaling, Remote Sensing, and GIS. Available online: http://www.citeulike.org/group/7954/article/4257773 (accessed on 20 September 2017).
37. Wu, J. Effects of changing scale on landscape pattern analysis: Scaling relations. *Landsc. Ecol.* **2004**, *19*, 125–138. [CrossRef]
38. Weng, Q.; Lu, D.; Schubring, J. Estimation of land surface temperature–vegetation abundance relationship for urban heat island studies. *Remote Sens. Environ.* **2004**, *89*, 467–483. [CrossRef]
39. Hang, J.; Li, Y. Ventilation strategy and air change rates in idealized high-rise compact urban areas. *Build. Environ.* **2010**, *45*, 2754–2767. [CrossRef]
40. Morris, K.I.; Chan, A.; Ooi, M.C.; Oozeer, M.Y.; Abakr, Y.A.; Morris, K.J.K. Effect of vegetation and waterbody on the garden city concept: An evaluation study using a newly developed city, Putrajaya, Malaysia. *Comput. Environ. Urban Syst.* **2016**, *58*, 39–51. [CrossRef]
41. Sun, R.; Chen, L. How can urban water bodies be designed for climate adaptation? *Landsc. Urban Plan.* **2012**, *105*, 27–33. [CrossRef]
42. Dubois, C.; Cloutier, G.; Rosenkilde Rynning, K.M.; Adolphe, L.; Bonhomme, M. City and building designers, and climate adaptation. *Buildings* **2016**, *6*, 3. [CrossRef]
43. Stone, B.; Vargo, J.; Habeeb, D. Managing climate change in cities: Will climate action plans work? *Landsc. Urban Plan.* **2012**, *107*, 263–271. [CrossRef]
44. Hebbert, M.; Jankovic, V. Cities and climate change: The precedents and why they matter. *Urban Stud.* **2013**, *50*, 1332–1347. [CrossRef]
45. Ren, C.; Cai, M.; Wang, R.; Xu, Y.; Ng, E. Local climate zone (LCZ) classification using the world urban database and access portal tools method: A case study in wuhan and hangzhou. In Proceedings of the Fourth International Conference on Countermeasure to Urban Heat Islands, Stephen Riady Centre, University Town, Singapore, 30 May–1 June 2016.
46. Stone, B.; Vargo, J.; Liu, P.; Hu, Y.; Russell, A. Climate change adaptation through urban heat management in Atlanta, Georgia. *Environ. Sci. Technol.* **2013**, *47*, 7780–7786. [CrossRef] [PubMed]